Jurnal Kejuruteraan 35(1) 2023: 65-76
https://doi.org/10.17576/jkukm-2023-35(1)-07

Samarium Doped Ceria (SDC) Electrolyte Modification by Sintering Aids Addition to Reducing Sintering Temperature: A Review

J. Zolhafizi[a], M. Azham Azmi[a*], H.A. Rahman [a], H. Zakaria[a], S. Hassan[a], S. Mahzan[a], A. Ismail[a], A.M.T. Ariffin[a], Tukimon M.F. [a], U.A. Yusof[a] & N. A. Baharuddin[b]

[a]*Faculty of Mechanical and Manufacturing Engineering, University of Tun Hussein Onn Malaysia, 86400 Parit Raja, Johor, Malaysia,*
[b]*Fuel Cell Institute, Universiti Kebangsaan Malaysia, 43600, UKM Bangi, Selangor, Malaysia*

**Corresponding author: azham@uthm.edu.my*

Received 25 November 2021, Received in revised form 25 April 2022
Accepted 27 May 2022, Available online 30 January 2023

ABSTRACT

The solid oxide fuel cell (SOFC) is a promising technology with specific characteristics for generating electricity by using hydrogen and oxidant as fuel. Typically, SOFC's use Samarium doped Ceria (SDC) as an electrolyte material as the ionic conductivity of SDC was better at lower operating temperatures which are below than 700°C that making it a good option for low and moderate temperature applications for SOFC. However, SDC electrolytes are cannot be densified below 1500°C. If a densified ceria-based electrolyte can be prepared at lower temperatures it can be co-sintered with another electrode component. This simplifies the fabrication process and reduces the cost. Other than that, it can help with porous electrode microstructure control and avoiding phase diffusion and chemical interaction problems. As a result, decreasing the sintering temperature may be another step toward commercialising SOFC technology. The modification of electrolyte by adding sintering aid was found as an effective method to lowering the sintering temperature. This paper, therefore, focuses on reviewing the attempts made to modify SDC electrolyte by adding sintering aid (Li_2O, CoO, CuO and FeO) in order to lowering sintering temperature. The studies related to temperature reduction, relative density, the microstructure of grains and conductivity of electrolyte was critically reviewed.

Keywords: SOFC; SDC; sintering temperature; sintering aid; electrolyte

INTRODUCTION

Solid oxide fuel cell (SOFC) technology faces the challenge of commercialization due to the high fabrication cost of SOFC components. One of the crucial stages in fabricating and manufacturing SOFC components is the sintering process. The sintering process needs to be controlled as to ensure ceramics products are well densified at the macro levels, therefore yielding products of excellent properties. The densification of the functional advanced ceramics often affects properties such as the microstructure, mechanical properties as well as electrical conductivity (Naceur et al. 2014; Rödel et al. 2009; Sturm & Jančar 2014; Toor & Croiset 2020). With regards to SOFC technology, the main challenge is the densification of the high-performance electrolyte such as samarium doped ceria (SDC) at low temperature (400-700C). The high sintering temperature is often unfavourable as this will incur high fabrication cost (Baertsch et al. 2004).

Generally, two primary ways have been thoroughly researched to enhance the sinterability of SOFC electrolytes. The first strategy is to use various powder preparation methods, such as mechanical milling, as well as chemical combustion vapour system or co-precipitation of oxalate (Herring 1950; Hwang et al. 2006; Lee & Choi 2004; Palmero 2015; Z. Wang et al. 2011). Another method is to apply sintering aids to promote the grain growth of electrolyte (Accardo et al. 2018; Dong et al. 2010, 2011; Fu et al. 2010; German & Rabin 1985; Gil et al. 2006; Le et al. 2013; Lima et al.2015; Santos et al. 2018; Sudarsan & Krishnamoorthy 2018; Villas-Boas et al. 2014; Zajac et al. 2009; T. S. Zhang et al. 2004; X. Zhang et al. 2006; Zhu et al. 2014). The atomic diffusivity of a basic material's grain boundary will change in the existence of sintering aids, resulting in a closed packing as shown in Figure 1. Metal oxide such as copper oxide was among the elements that had been proved to enhance the atomic diffusivity of material (Lima et al. 2015). Thus, Metal oxide can be incorporated into SOFC electrolyte materials as additive that effectively lower the sintering temperature. This factor would significantly reduce the energy and time required for sintering process.

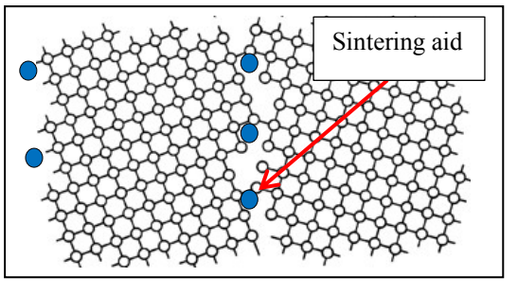

FIGURE 1. Sintering aid atom diffuse into the grain boundary of primary material.

The ionic conductivities of 20 mol percent samarium doped cerium oxide ($Sm_{0.2}Ce_{0.8}O_{1.9}$, SDC) as an electrolyte for solid oxide fuel cells in intermediate temperatures are among the highest, however it is limited to commercial use due to its poor densification behavior (Kim 1989; Le et al. 2013; Shi et al. 2020). In order to overcome the higher densification temperature of SDC, which is above 1500°C, the use of sintering aid as an additive had been actively conducted. Sintering aids are functional additives or dopants that lead to the enhancement of the performance of densifying mechanism (Azham Azmi et al. 2019; Muda et al. 2019; Yahya et al.2014). There are many materials that have been used as a sintering aid for SDC electrolyte such as bismuth, titanium, iron, copper, manganese, lithium and cobalt. The most common transition metals explored as sintering aids for doped ceria are lithium, cobalt, copper, and iron (Table 1). (Dong et al. 2010, 2011; Le et al. 2013; Lima et al. 2015; Nicholas & De Jonghe 2007; Santos et al. 2018; Zajac et al. 2009; T. S. Zhang et al. 2004; X. Zhang et al. 2006; Zhu et al. 2014).

There are four sections to this article: The first is concerned with the degree of sintering temperature reduce for SDC when co-doped with sintering aid. The second section describes the effect of sintering aids toward relative shrinkage and relative density of SDC which determine the optimum sintering temperature for SDC. The third section deals with the microstructures change for co-doped SDC in term of grain size and the size of pore between the grain which determine the porosity of the material. The last section determine the conductivity of co-doped SDC which improves the electrolyte's total electrical conductivity by enhancing oxygen vacancy content in the grain boundary and lowering oxygen vacancy depletion in the space charge layers (Han et al. 2011).

SINTERING TEMPERATURE REDUCE

The main purpose of sintering aids is to lowering down the extravagant sintering temperature of SDC which cause the high consume of energy along with the operational costing. In the past decades, many researches had been conducted in order to identify the suitable sintering aids as an additive towards SDC. Table 1 show that the summary of preferred choice of sintering aids used in previous researches which are lithium oxide (Li_2O), cobalt oxide (CoO), copper oxide (CuO) and iron oxide (FeO).

From the table, the amount of sintering aids and their ability to reducing the sintering temperature of SDC which is originally at 1500°C was summarized and tabulated. Based on the result, the amount of Li_2O used as a dopant was higher compared to others with concentration between 2.0-2.5 mol% where the sintering temperature of SDC can be minimized to 1200-900°C. Other than that, CoO and FeO as a sintering aids for SDC were conducted by using only a small amount of concentration which were 0.25-3.0 mol% and 0.25-1.5 mol% respectively. Both sintering aids can minimize the sintering temperature for SDC to 1400-800°C for CoO and 1400-1200°C for FeO. The last sintering aids had been studied was CuO. Although the concentration of CuO used as a sintering aid for SDC is slightly higher compare to CoO and FeO with 0.5-2.0 mol%, when compared to other sintering aids, the sintering temperature drop range was the lowest, with 1100-750°C. As a whole, CuO can be considered as the best sintering aid for SDC compared to Li_2O, CoO and FeO to lowering sintering temperature.

TABLE 1. Concentration of sintering aids and temperature reduce of co-doped SDC from 1500°C

No	Sintering Aids	Wt%	Temperature Reduce (from 1500°C)	Article
1.	Lithium Oxide (Li_2O)	2.0-2.5 mol	1200-900	(Han et al. 2011; Kim, 1989; Le et al. 2013; Preethi et al. 2019; Zhu et al. 2014)
2.	Cobalt Oxide (CoO)	0.25-3.0 mol	1400-800	(Chen et al. 2012; Fu et al. 2010; Varela et al. 1999; Yoshida & Inagaki, 2006; T. Zhang et al. 2002; X. Zhang et al. 2006)
3.	Copper Oxide (CuO)	0.5-2.0 mol	1100-750	(Dong et al. 2010, 2011; Lima et al. 2015; Santos et al. 2018; Toor & Croiset, 2020; Zajac et al. 2009; X. Zhang et al. 2006)
4.	Iron Oxide (FeO)	0.25-1.5 mol	1400-1200	(Arunkumar et al. 2014; Ding et al. 2019; Fu et al. 2010; Sudarsan & Krishnamoorthy, 2018; Zajac et al. 2009; T. S. Zhang et al. 2004)

RELATIVE SHRINKAGE AND DENSITY

The ratio of a substance's density (mass per unit volume) to the density of a specified reference material is known as relative shrinkage and density, or specific gravity. The optimum sintering temperature for SDC electrolyte occur at the higher relative density which were agreed at 1500°C with relative density of 97.3% (Khan & Akhtar 2019; Yin et al. 2014). SDC and Li-SDC sintered shrinkage and shrinkage rate at different heating rates were shown in Figures 2 and 3. As the heating rate rose, it causes the increasing of maximum shrinkage rate. As a slower heating rate was employed to obtain the similar temperature, a lengthened scale of time for mass diffusion and transport can be attributed.

Figures 2 and 3 indicate that the Li-SDC reached nearly full density at nearly 900°C, whereas the SDC only reached 81.5%. Furthermore, at 10°C min^{-1}, the highest shrinkage rate for Li-SDC was 1.1 min^{-1}, but it was only $4.6x10^{-3}$ min^{-1} for SDC, which was only around 0.4% of Li-SDC. This showed the sintering aid's effectiveness of lithium oxide. At 898°C with 3°C min^{-1}, 953°C with 5°C min^{-1}, and 1048°C with 10°C min^{-1}, the Li-SDC achieved a density of 99.5%, according to Figure 3(a). SDC on the other hand, even when sintered at 1250°C, a density of only 82% was reached, regardless of the heating rate. Lithium oxide doping has a very obvious effect. With the addition of lithium oxide, the beginning of sintering was accelerated. Sintering was forwarded from 600°C to 500°C at 5°C min^{-1} of heating rate, for example. It's likely that the gradient in chemical potential between the particle neck and the surface rose as a result of the addition of lithium oxide, increasing CeO2 atom flux (Le et al. 2013).

For different Co concentrations, Figure 4A illustrates the linear shrinkage rate versus temperature. 1% Co-doped sample exhibits a similar shrinkage trend to that of 0.25% Co-doped. For clarity, the curve for 1% Co doping is omitted. The inclusion of Co pushes the initiation of sintering towards lower temperatures, as can be seen in this figure. Furthermore, a modest value of Co-doped significantly lowers the maximum shrinkage rate temperature. As an example, the maximum shrinkage rate for pure ceria drops to 1214°C for 0.25% Co-doped SDC at 1428°C. The difference in maximum shrinkage rate values between the two samples is greater than 200°C. Findings indicate that 0.25% Co doping lowers sintering temperatures by more over 200°C. However, as the doping level rises in the total Co concentration, the values of maximum shrinkage rate drop. As demonstrated below, it could be related by the action of blocked pores in grain interiors and along grain borders. 15 K/min was used as a higher heating rate to prevent completing the greatest densification throughout the temperature ramp. Figure 4B shows the results. Undoped ceria densifies slowly at 1300°C, and this sample produces just 87% relative density after 2 hours. However, a 0.25% Co-doped sample densifies quickly, reaching over 99.0% relative density after only 2 hours at 1300°C. This density is greater than that of pure CeO_2 sintered for 2 hours at 1525°C (Yoshida & Inagaki 2006; T. Zhang et al. 2002; X. Zhang et al. 2006).

Figure 5 shows the results of a study done by X. Zhang et al. 2006, to determine the sintering behaviour of Co-SDC or Cu-SDC. The addition of sintering aids lowers the sintering curve from 1100°C (SDC) to 800°C (Co-SDC) and 750°C (Cu-doped), boosting densification considerably. For both Co and Cu addition, rising the concentration from 1% to 5% shows a modest influence on the behaviour of densification. The linear shrinkage rate as a function of temperature is shown in Figure 5B. This graph illustrates that the maximum shrinkage rate varies according on the dopant type, for SDC at 1290°C with 0.58°C^{-1}, for Co-SDC at 913–975°C with 0.70–0.72°C^{-1}, and for Cu-SDC at 920°C with 1.1°C^{-1}. The difference in temperature between SDC's maximum shrinkage rate and sintering aids addition is higher than 200°C. Furthermore, inclusion of sintering aids considerably improves the SDC's densification rate. Cu-SDC is more effective than the two sintering aids. With Co or Cu assistance, the liquid phase and viscous flow sintering procedures lead to a huge decrease in sintering temperature (X. Zhang et al. 2006).

The result for the relative density of FeO was shown in Figure 6. Both ceria and SDC undergo solid state sintering at 1200°C without sintering aid, resulting in similar but lesser densification. The material attempts to minimize the surface energy during solid state sintering, causing the growth of grain. Development of grain initially occurs with the production of a neck at the grain interface, and the resulting pores between the grains close to form a network, resulting in a density rise during sintering. For SDC, compared to pure oxide, the addition of samarium ions inhibits the formation of interfacial necks between ceria grains by altering the grain's surface energy. As a result, when compared to ceria, a slight decrease of SDC's density (83%) was seen during sintering (86%). The iron functions as a sintering aid in FDC (Fe-ceria) and FSDC (Fe-SDC) and promotes densification at a lower sintering temperature of 1200°C. The smallest change in strain value and lattice parameter was recorded after sintering, indicating iron segregation in the ceria and SDC grain boundary (Arunkumar et al. 2014). The segregated iron result in a consistent viscous flow of iron oxide occurs throughout the material. The capillary force is induced, driving the viscous flow of iron oxide throughout the grain boundary and cause a thin amorphous metal oxide film between the grains, reducing friction. The lower friction, grain boundary sliding increases, potentially resulting in compact grain rearrangement and decreasing the pores of grain boundary. SDC with 0.5 mol% iron resulted in higher densication (98%) when sintering at 1200°C, however SDC with 1.5 mol% iron results in a little reduction in relative density compared to 0.5 mol% iron. In 1.5FSDC and 1.5FDC, a greater sintering aid concentration causes rapid grain development, which makes pore closure more difficult, resulting in a lower density (Arunkumar et al. 2014).

Table 2 shows the summary of relative density and maximum shrinkage rate for selected electrolyte. From the table, Li-SDC, Co-SDC, Cu-SDC and Fe-SDC shows the increment in relative density compared to SDC when undergo sintering process at temperature between 1000°C to 1400°C. Among the electrolyte selected, Li-SDC, Co-SDC and Cu-SDC show the highest relative density with 99% while Fe-SDC just slightly lower with 98%. Other than that, Cu-SDC show the highest maximum shrinkage rate compares to other electrolyte at 920°C with 1.1°C^{-1}. Even though, Li-SDC have similar maximum shrinkage rate with Cu-SDC, Cu-SDC was the best because it occurs at lower temperature compared to Li-SDC. In summary, copper can be considered as the best sintering aid for SDC electrolyte in term of relative density and maximum shrinkage rate compared to the others.

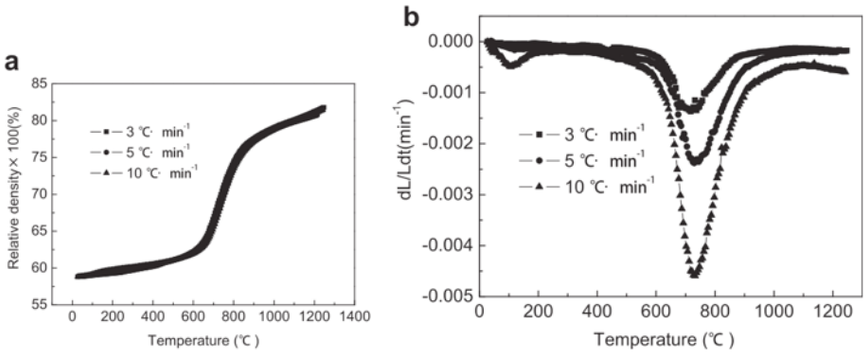

FIGURE 2. Constant heating rate sintering of SDC (a) Relative density as a function of temperature, (b) Shrinkage rate as a functional of temperature(Le et al. 2013).

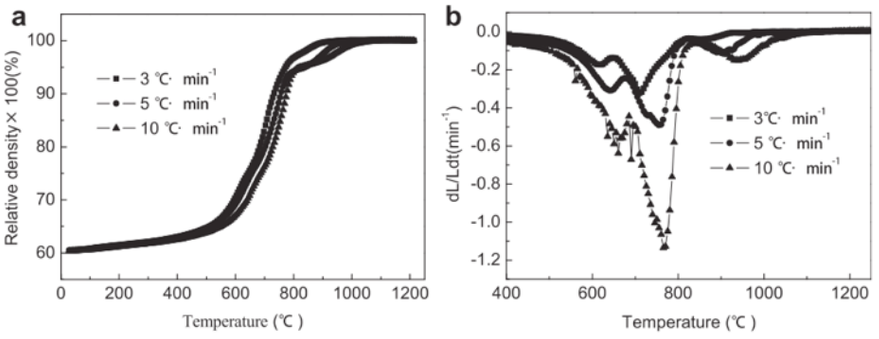

FIGURE 3. Constant heating rate sintering of Li-SDC (a) Relative density as a function of temperature, (b) Relative shrinkage rate as a functional of temperature (Le et al. 2013).

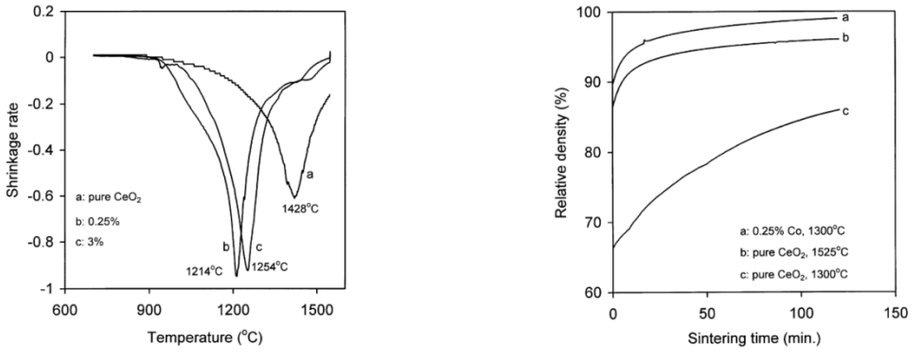

FIGURE 4. (A) Shrinkage rate against sintering temperature for (a): pure ceria, (b): 0.25% and (c): 3.0% Co-doped ceria sintered at a heating rate of 10 K/min. (B) Effect of sintering time and temperature on the density of undoped and 0.25% Co-doped ceria (T. Zhang et al. 2002).

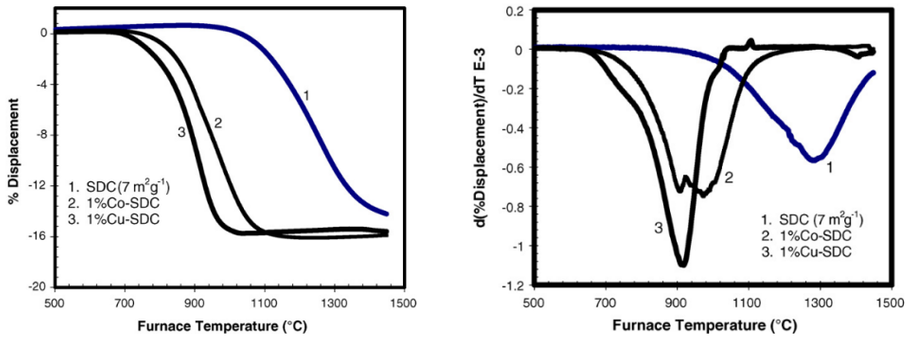

A B

FIGURE 5. (A) Linear shrinkage (displacement%) vs. sintering temperature at a heating rate of 5°Cmin^{-1}. (B) Linear shrinkage rate vs. sintering temperature at a heating rate of 5°Cmin^{-1}(X. Zhang et al. 2006).

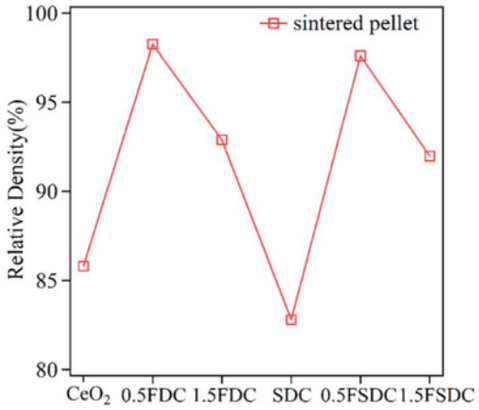

FIGURE 6. Relative density of the CeO_2, SDC and FSDC (Arunkumar et al. 2014).

TABLE 2. Summary of relative density and maximum shrinkage rate for selected electrolyte

No	Electrolyte	Relative Density (at 1000-1400°C)	Maximum Shrinkage Rate	Article
1.	SDC	~81.5%	0.58°C^{-1} at 1290°C	(Le et al. 2013), (X. Zhang et al. 2006), (Arunkumar et al. 2014)
2.	Li-SDC	~99%	1.1°C^{-1} at 953°C	(Han et al. 2011; Kim, 1989; Le et al. 2013; Preethi et al. 2019; Zhu et al. 2014)
3.	Co-SDC	~99%	0.72°C^{-1} at 975°C	(Chen et al. 2012; Fu et al. 2010; Varela et al. 1999; Yoshida & Inagaki, 2006; T. Zhang et al. 2002; X. Zhang et al. 2006)
4.	Cu-SDC	~99%	1.1°C^{-1} at 920°C	(Dong et al. 2010, 2011; Lima et al. 2015; Santos et al. 2018; Toor & Croiset, 2020; Zajac et al. 2009; X. Zhang et al. 2006)
5.	Fe-SDC	~98%	0.5°C^{-1} at 989°C	(Arunkumar et al. 2014; Ding et al. 2019; Fu et al. 2010; Sudarsan & Krishnamoorthy, 2018; Zajac et al. 2009; T. S. Zhang et al. 2004)

MICROSTRUCTURE

Microstructure including anode, cathode and electrolyte is required by the fuel cell's functional principle. Since the function of electrolyte is to separate the fuel and oxidant as two different gas compartments, it must be gas-tight. As a result, the electrolyte layer must be dense and porous. As the gas-tightness is maintained, with a given bulk ion conductivity of the material, the electrolyte layer can be as thin as feasible to reduce electrical resistance (Hussain & Yangping 2020; Menzler et al. 2010; Shi et al. 2020; F. Wang et al. 2019; Zakaria et al. 2020). Microstructure of SDC increases in grain size during the sintering process. According to previous study, the average SDC grain size was around 770 nm, and the SDC grain was extremely porous (Arabacı 2020; Dai et al. 2020; Yin et al. 2014).

The SDC's microstructures with and without sintering aids varied considerably with sintering time at 1500°C, according to Yoshida & Inagaki (2006). SEM pictures of SDC without sintering aids manufactured at 1500°C for varied sintering periods are shown in Figure 7. SDC grains grew with sintering time at 1500°C, which was proven. However, even after 24 hours of sintering, little grains of practically the same size as calcined powder and some big pores were discovered. As previously reported, dense SDC proved difficult to achieve by sintering at 1500°C from calcined powder generated using a standard solid-state reaction technique (Yoshida & Inagak, 2006).

All compositions demonstrated excellent microstructure when sintered at 1400°C for 6 hours or 1450°C for 4 hours. However, after 6 hours of sintering at 1450°C, considerable porosity was discovered, and this oversintering had a negative impact on the overall conductivity, particularly of the undoped SDC. At 3°C min^{-1} of heating rate, Figure 8 depicted the size of grain evolution of SDC and Li-SDC. When the density was less than 82% at 700°C, the average grain size of Li-SDC remained the same, but it rose fast with the increase of relative density. At 950°C, 0.35 µm was measured. At 700°C with relative density less than 70%, however, the grain size of SDC remained practically unchanged, and then grew after that. When sintered at 1300°C, it reached 0.22 µm, with a relative density of only 82% (Le et al. 2013).

Figure 9 displays SEM pictures of Co-SDC after being heated to 1500°C for 10 minutes and then for 24 hours. The composite demonstrated initiation of grain growth even after sintering at 1500°C for 10 minutes, and at grain borders the pores become concentrated. As for Co-SDC, all grains grew. Co_3O_4 was thought to increase grain development during the early stages of sintering, based on Figure 9. All samples were densely sintered after 24 hours of sintering at 1500°C, however some pores remained in the grains, indicating that grain boundaries move significantly quicker than pores (Yoshida & Inagaki 2006).

The influence of sintering temperature and duration on the microstructure of SDC and 0.25% Co-SDC samples is shown by T. Zhang *et al.* 2002. The size of grain of SDC sintered at 1300°C is roughly 0.7µm, which is greater than before sintered (0.4µm). When sintered at 1300°C with 0.25% Co-SDC is substantially denser with 11.7 µm grain size compare SDC sintered at 1525°C with no doping (5.3 µm). These findings show that a little quantity of Cobalt additive significantly increased densification and enhances grain boundary movement (T. Zhang et al. 2002).

Figure 10 shows SEM images of pure SDC, copper doped SDC (xCu-SDC, x=0.1,0.5,1.0,3.0,5.0) sintered for 5 hours at 1100°C in air. The image of SEM for SDC (Figure 10a) in Figure 10 is with the magnification of 10k and the rest with the magnification of 5k. SDC used 10k magnification because the grain size was quite smaller which cause surface characteristics less observable when using lower magnifications. Except for SDC and 0.1-Cu-SDC, all samples in Figure 10 have an extremely thick microstructure. Grain size distribution and form are similar in samples with 0.5 mol% copper and above, with larger grains (2 µm) and smaller grains (less than 1 µm). Figure 11 shows a SEM picture of SDC sintered for 5 hours at 1350°C in the air for comparison. Figure 11 illustrates that SDC samples do not fully densify even at 1350°C (pores present on the surface). The tiny size of grain (near to 200nm) is another indicator that the sample has not yet completed full sintering. Figure 10 shows that 0.5 mol% copper is adequate to produce maximum densification for 5 hours at 1100°C, since copper with higher concentrations result in similar microstructure (Toor & Croiset 2020).

Last but not least, the research regarding the used of iron (FeO) as sintering aids was investigated. The SEM result of sintered SDC's microstructure, 0.5Fe-SDC, and 1.5Fe-SDC is shown in Figure 12(a–c). The poor sintering of sintered SDC at 1200°C is indicated by the strong porosity microstructure on the surface (Figure 12(a)). Because SDC undergoing sintering at solid phase, complete densication necessitates high sintering temperature which is higher than 1400°C. In the case of sintered xFe-SDC, however, the surface often exhibits a dense microstructure with an average size of 100-500nm, as well as small pinholes indicating the material undergoing complete sintering by sintering aid's viscous flow around the core of grain boundary (Arunkumar et al. 2014; T. S. Zhang et al. 2004).

Table 3 show the summary of grain size for selected electrolyte at temperature of 1000 to 1400°C. The results show that the entire SDC electrolyte that had been doped with sintering aids was undergoing the growth of grain size. The grain of Li-SDC increase slightly compare to pure SDC with increment of 0.13 µm from 0.22 µm of pure SDC size. The other type of electrolyte shows higher grain size compare to Li-SDC with 0.5 µm (Fe-SDC), 2 µm (Cu-SDC) and 11.7 µm (Co-SDC). The larger the grain, the less closed pack between the grains and the more sintering aid's viscous flow along the grain boundary, indicating complete sintering of the material. Finally, it may be concluded that cobalt is the best sintering aid for SDC in term of grain size increment.

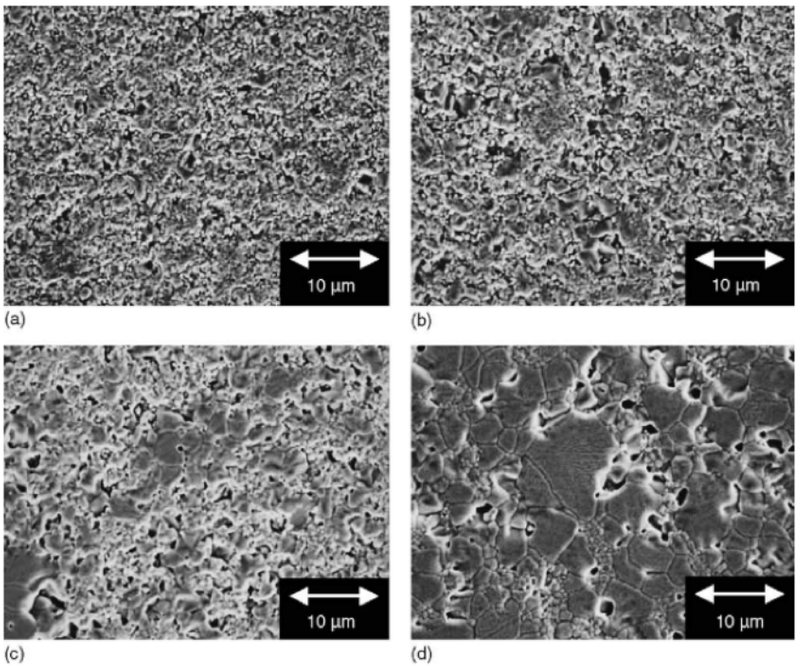

FIGURE 7. SEM images of SDC sintered at 1500°C: (a) 10 min, (b) 1 h, (c) 5 h and (d) 24 h (Yoshida & Inagaki 2006)

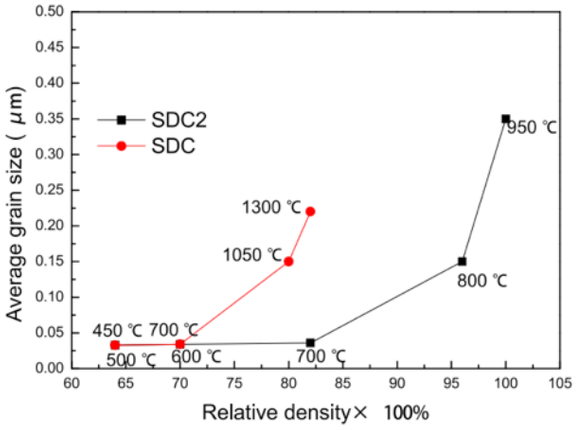

FIGURE 8. Grain size of SDC and Li-SDC during sintering at a heating rate of 3°C min^{-1} (Le et al. 2013)

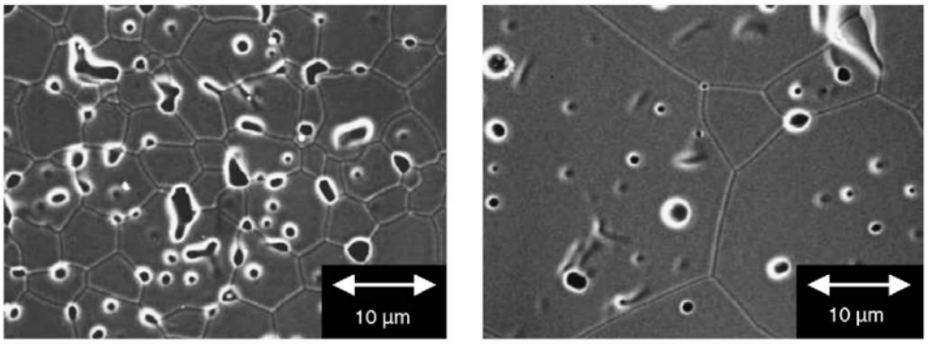

FIGURE 9. SEM images of Co-SDC sintered at 1500°C, (a) 10 min, (b) 24 h, (Yoshida & Inagaki 2006).

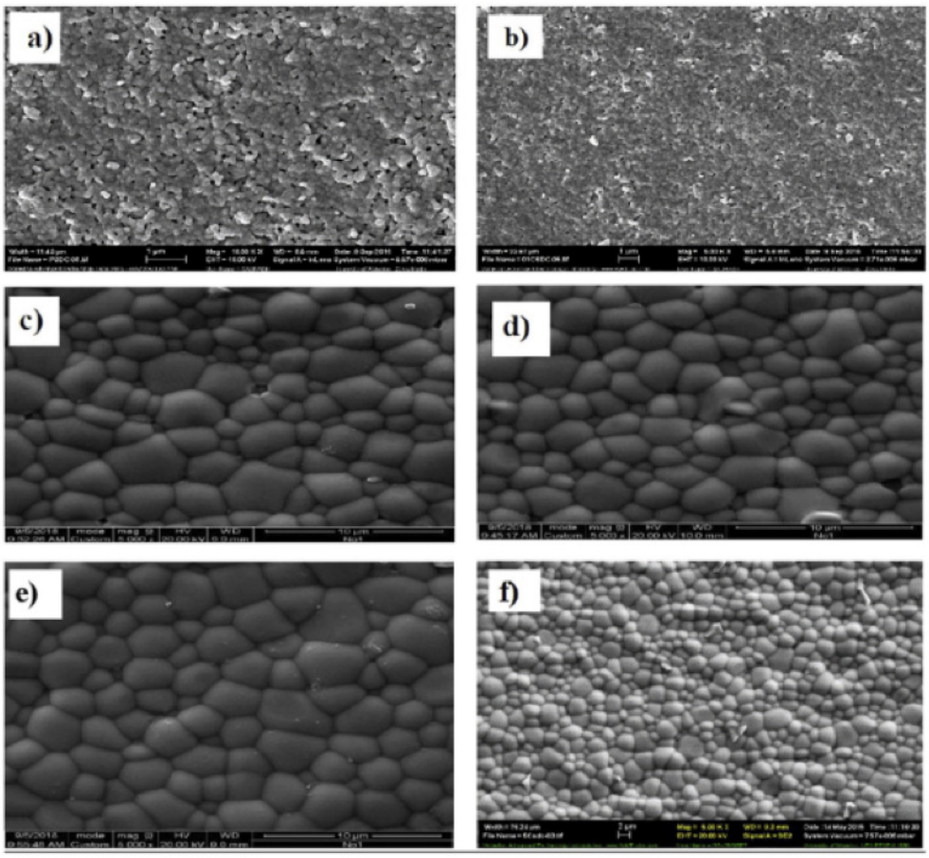

FIGURE 10. SEM images of electrolyte samples sintered at 1100 °C; a) Pure SDC, b) 0.1- Cu-SDC, and c) 0.5- Cu-SDC, d) 1.0- Cu-SDC, e) 3.0- Cu-SDC, and f) 5.0- Cu-SDC (Toor & Croiset 2020).

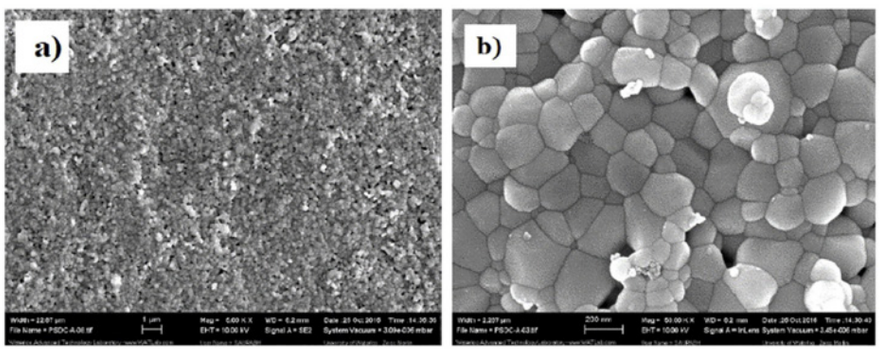

FIGURE 11. SEM of SDC samples sintered at 1350 °C; a) 5k and b) 50k (Toor & Croiset 2020)

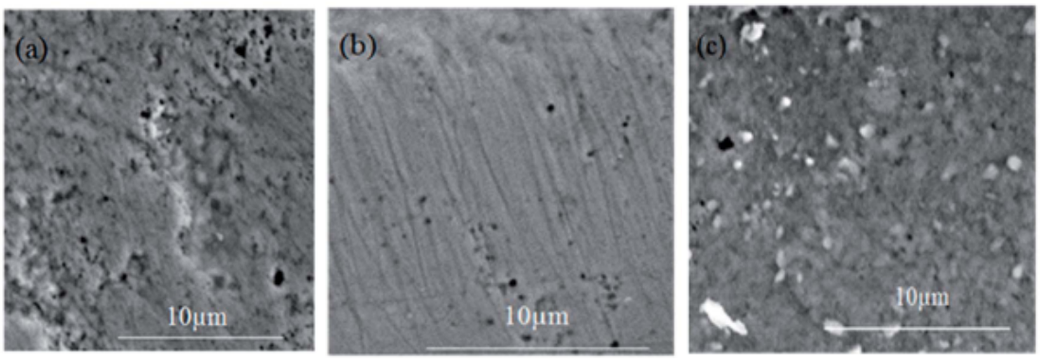

FIGURE 12. SEM images showing microstructure (a) SDC (b) 0.5Fe-SDC and (c) 1.5Fe-SDC sintered at 1200°C (Arunkumar et al. 2014)

TABLE 3. Summary of grain size for selected electrolyte at temperature of 1000 to 1400°C.

No	Electrolyte	Grain Size (at 1000-1400°C)	Article
1.	SDC	0.22 µm	(Toor & Croiset, 2020), (Le et al. 2013), (T. Zhang et al. 2002), (Yoshida & Inagaki, 2006), (Arunkumar et al. 2014), (Yin et al. 2014)
2.	Li-SDC	0.35 µm	(Han et al. 2011; Kim, 1989; Le et al. 2013; Preethi et al. 2019; Zhu et al. 2014)
3.	Co-SDC	11.7 µm	(Chen et al. 2012; Fu et al. 2010; Varela et al. 1999; Yoshida & Inagaki, 2006; T. Zhang et al. 2002; X. Zhang et al. 2006)
4.	Cu-SDC	2 µm	(Dong et al. 2010, 2011; Lima et al. 2015; Santos et al. 2018; Toor & Croiset, 2020; Zajac et al. 2009; X. Zhang et al. 2006)
5.	Fe-SDC	0.5 µm	(Arunkumar et al. 2014; Ding et al. 2019; Fu et al. 2010; Sudarsan & Krishnamoorthy, 2018; Zajac et al. 2009; T. S. Zhang et al. 2004)

CONDUCTIVITY

The operational temperature of SOFCs is generally determined across electrolyte's ionic conduction caused by the movement of oxygen ions via oxygen vacancies. In recent years, it has been recognised that 20% doped-ceria solid is the best electrolyte for intermediate-temperature fuel cells between 500°C to 600°C, because of the higher ionic conductivity compare to previously yttria-stabilized zirconia (YSZ) materials with operating temperatures of 1000°C (Ding et al. 2019; Kosinski & Baker 2011; Tian et al. 2020; Yusop et al. 2020). It should be emphasised, however, that at intermediate temperatures, the grain boundary behaviour frequently dominates the total conductivity of a solid electrolyte. The particular grain border conductivity in typical polycrystalline YSZ has been reported to be several orders of magnitude lower than the grain interior conductivity. The existence of thin siliceous layers is largely responsible for the blocking action of grain boundaries. For decades, detrimental grain boundary behaviour caused by silica oxide impurity has been known in zirconia-based electrolytes, and for over a decade in ceria-based ceramics (T. S. Zhang et al. 2004).

In precursor materials, the presence of SiO_2 impurity is common. SiO_2 contamination can also come from high-temperature sintering furnace refractories, as well as the apparatus that used silicone grease for establishing input gas mixes for cell test assemblies of fuel cell. Thus, removing the grain boundaries negative effect on conductivity in total is difficult. Therefore, numerous efforts to decrease the grain boundary effect have been made using different sintering aids such as Al_2O_3, TiO_2 and Bi_2O_3. Al_2O_3 has been shown to be the best sintering aids for enhancing the conductivity of grain boundary of zirconia-based electrolytes thus far. However, earlier research has shown that adding Al_2O_3 to doped-ceria reduces both grain border and grain interior conductivities caused by the creation of a new phase, $GdAlO_3$ (T. S. Zhang et al. 2004).

Metal oxides, such as LiO_2, CoO, CuO, and FeO, are good additives for ceria ceramics, as previously described (Dong et al. 2010, 2011; Le et al. 2013; Lima et al. 2015; Nicholas & De Jonghe 2007; Santos et al. 2018; Zajac et al. 2009; T. S. Zhang et al. 2004; X. Zhang et al. 2006; Zhu et al. 2014). LiO_2, CoO, CuO, had a negative impact on the ceria ceramics' grain boundary conductivity as they encouraged the propagation of silica oxide at the borders of the grain. LiO_2, CoO, and CuO as additives for ceria ceramics are not acceptable in this regard. In contrast, FeO is the best additives and provides the ability to scavenge of silica oxide impurity in ceria-based electrolytes.

The influence of sintering temperature on the conductivities of Fe-doped ceria with 0.5 at.% Fe has also been investigated. The best sintering temperature for Fe-doped ceria with 0.5 at.% to obtain the greatest total conductivity is 1450°C, as illustrated in Figure 13, as opposed to 1600°C for the undoped ceria. As a result of the electrical measurements, iron doping can lower the temperature of sintering. Other than that, differ from undoped samples, the grain interior conduction controls the fluctuation in total conductivity with sintering temperature in the 0.5 at.% Fe-doped ceria, implying that the grain boundary conduction greatly inhanced with addition 0.5 at.% of iron oxide. Although sintering temperatures between 1400 and 1600°C have no discernible effect on grain boundary conductivity, the ideal sintering temperature must be between 1400°C and 1500°C since sintering temperatures beyond 1500°C result in a considerable reduce in grain interior conductivity. This is due to the fact that higher sintering temperatures allow more Fe^{3+} ions to enter the doped grains. (T. S. Zhang et al. 2004).

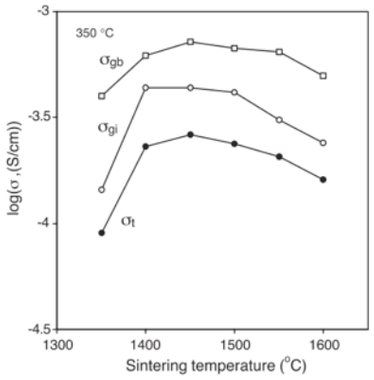

FIGURE 13. Effect of sintering temperature on the conductivities of the 0.5 at.% Fe-doped ceria (σ_{gb}, σ_{gi} and σ_t, stand for the grain boundary, grain interior and total conductivities) (T. S. Zhang et al. 2004).

SUMMARY AND CONCUSION

Lithium, cobalt, copper and iron have been the most popular ceramic oxide studied as sintering aids for doped ceria. Referring to Table 4, SDC co-doped with 0.5-2.0 mol% CuO can be considered as the best sintering aid for electroyte as it can lowering the sintering temperature to the range of 1100-750°C which was the lowest compared to Li_2O, CoO and FeO. Cu-SDC also have better relative density and maximum shrinkage rate compared to other electrolyte. Other than that, this review found that Co-SDC have bigger grain size compared to Li-SDC, Cu-SDC and Fe-SDC. Nevertheless, in term of conductivity, FeO has the better conductivity compared to others because it can block the propagation of SiO2 impurities.

TABLE 4. Summary of Sintering Aids

No	Sintering Aids	Wt%	Temperature Reduce (°C)	Propagation of SiO_2 impurities	Conductivity
1.	Lithium Oxide (Li_2O)	2.0-2.5 mol	1200-900	Promote	Good
2.	Cobalt Oxide (CoO)	0.25-3.0 mol	1400-800	Promote	Good
3.	Copper Oxide (CuO)	0.5-2.0 mol	1100-750	Promote	Good
4.	Iron Oxide (FeO)	0.25-1.5 mol	1400-1200	Block	Best

ACKNOWLEDGEMENT

The authors gratefully acknowledge the financial support provided by Malaysia Ministry of Education through Fundamental Research Grant Scheme (FRGS) - K317, and Research Management Centre (RMC), Universiti Tun Hussein Onn Malaysia (UTHM) for managing our research grant.

DECLARATION OF COMPETING INTEREST

None

REFERENCES

Accardo, G., Frattini, D., Ham, H. C., Han, J. H. & Yoon, S. P. 2018. Improved microstructure and sintering temperature of bismuth nano-doped GDC powders synthesized by direct sol-gel combustion. *Ceramics International* 44(4): 3800–3809. DOI:https://doi.org/10.1016/j.ceramint.2017.11.165.

Arabacı, A. 2020. Effect of the calcination temperature on the properties of Sm-doped CeO2. *Emerging Materials Research* 9(2): 296–301. DOI:https://doi.org/10.1680/jemmr.18.00082.

Arunkumar, P., Preethi, S. & Suresh Babu, K. 2014. Role of iron addition on grain boundary conductivity of pure and samarium doped cerium oxide. *RSC Advances 4*(84): 44367–44376. DOI:https://doi.org/10.1039/c4ra07781d

Azham Azmi, M., Mahzan, S., Ahmad, S., Salleh, S. M., Rahman, H. A., Choiron, M. A., Ismail, A. & Taib, H. 2019. Vibration exposure of polydimethylsiloxane (PDMS) reinforced silica (sio2): Comparison of different source of silica (sio2) as filler. *IOP Conference Series: Materials Science and Engineering 494*(1). DOI:https://doi.org/10.1088/1757-899X/494/1/012069.

Baertsch, C. D., Jensen, K. F., Hertz, J. L., Tuller, H. L., Vengallatore, S. T., Spearing, S. M. & Schmidt, M. A. 2004. Fabrication and structural characterization of self-supporting electrolyte membranes for a micro solid-oxide fuel cell. *Journal of Materials Research 19*(9): 2604–2615. DOI: https://doi.org/10.1557/JMR.2004.0350.

Chen, D., Wang, F. & Shao, Z. 2012. Interlayer-free electrodes for IT-SOFCs by applying Co 3O 4 as sintering aid. *International Journal of Hydrogen Energy 37*(16): 11946–11954. DOI:https://doi.org/10.1016/j.ijhydene.2012.05.053.

Dai, H., Kou, H., Tao, Z., Liu, K., Xue, M., Zhang, Q. & Bi, L. 2020. Optimization of sintering temperature for SOFCs by a co-firing method. *Ceramics International 46*(5): 6987–6990. DOI:https://doi.org/10.1016/j.ceramint.2019.11.134.

Ding, H., Qu, D., Sun, H., Guo, X., Li, J., Li, Q., Li, G., Wang, P. & Zhang, X. 2019. Improved sintering behavior and electrical performance of Ce0.8Sm0.2O2-δ - BaZr0.1Ce0.7Y0.2O3-δ (SDC-BZCY) composite electrolytes with the addition of iron (III) oxide for IT-SOFCs. *Ceramics International 45*(18): 24702–24706. DOI:https://doi.org/10.1016/j.ceramint.2019.08.209.

Dong, Y., Hampshire, S., Lin, B., Ling, Y. & Zhang, X. 2010. High sintering activity Cu-Gd co-doped CeO2 electrolyte for solid oxide fuel cells. *Journal of Power Sources 195*(19): 6510–6515. DOI:https://doi.org/10.1016/j.jpowsour.2010.03.053.

Dong, Y., Hampshire, S., Zhou, J. E. & Meng, G. 2011. Synthesis and sintering of Gd-doped CeO2 electrolytes with and without 1 at.% CuO dopping for solid oxide fuel cell applications. *International Journal of Hydrogen Energy 36*(8): 5054–5066. DOI:https://doi.org/10.1016/j.ijhydene.2011.01.030.

Fu, C. J., Liu, Q. L., Chan, S. H., Ge, X. M. & Pasciak, G. 2010. Effects of transition metal oxides on the densification of thin-film GDC electrolyte and on the performance of intermediate-temperature SOFC. *International Journal of Hydrogen Energy*, *35*(20): 11200–11207. DOI:https://doi.org/10.1016/j.ijhydene.2010.07.049.

German, R. M. & Rabin, B. H. 1985. Enhanced sintering through second phase additions. *Powder Metallurgy 28*(1): 7–12. DOI:https://doi.org/10.1179/pom.1985.28.1.7.

Gil, V., Tartaj, J., Moure, C. & Durán, P. 2006. Sintering, microstructural development, and electrical properties of gadolinia-doped ceria electrolyte with bismuth oxide as a sintering aid. *Journal of the European Ceramic Society 26*(15): 3161–3171. DOI:https://doi.org/10.1016/j.jeurceramsoc.2005.09.068.

Han, M., Liu, Z., Zhou, S. & Yu, L. 2011. Influence of Lithium Oxide Addition on the Sintering Behavior and Electrical Conductivity of Gadolinia Doped Ceria. *Journal of Materials Science and Technology*, *27*(5): 460–464. DOI:https://doi.org/10.1016/S1005-0302(11)60091-1.

Herring, C. 1950. Diffusional viscosity of a polycrystalline solid. *Journal of Applied Physics 21*(5): 437–445. DOI:https://doi.org/10.1063/1.1699681.

Hussain, S. & Yangping, L. 2020. Review of solid oxide fuel cell materials: cathode, anode, and electrolyte. *Energy Transitions 4*(2): 113–126. DOI:https://doi.org/10.1007/s41825-020-00029-8.

Hwang, C. C., Huang, T. H., Tsai, J. S., Lin, C. S. & Peng, C. H. 2006. Combustion synthesis of nanocrystalline ceria (CeO2) powders by a dry route. *Materials Science and Engineering B: Solid-State Materials for Advanced Technology 132*(3): 229–238. DOI:https://doi.org/10.1016/j.mseb.2006.01.021.

Khan, S. B. & Akhtar, K. 2019. *Cerium Oxide: Applications and Attributes*. BoD–Books on Demand.

Kim, D. -J. 1989. Lattice Parameters, Ionic Conductivities, and Solubility Limits in Fluorite-Structure MO2 Oxide [M = Hf4+, Zr4+, Ce4+, Th4+, U4+] Solid Solutions. *Journal of the American Ceramic Society 72*(8): 1415–1421. DOI:https://doi.org/10.1111/j.1151-2916.1989.tb07663.x.

Kosinski, M. R. & Baker, R. T. 2011. Preparation and property-performance relationships in samarium-doped ceria nanopowders for solid oxide fuel cell electrolytes. *Journal of Power Sources 196*(5): 2498–2512. DOI:https://doi.org/10.1016/j.jpowsour.2010.11.041.

Le, S., Zhu, S., Zhu, X. & Sun, K. 2013. Densification of Sm0.2Ce0.8O1.9 with the addition of lithium oxide as sintering aid. *Journal of Power Sources 222:* 367–372. DOI:https://doi.org/10.1016/j.jpowsour.2012.08.020.

Lee, J. S. & Choi, S. C. 2004. Crystallization behavior of nano-ceria powders by hydrothermal synthesis using a mixture of H2O2 and NH4OH. *Materials Letters 58*(3–4): 390–393. DOI:https://doi.org/10.1016/S0167-577X(03)00508-1.

Lima, C. G. M., Santos, T. H., Grilo, J. P. F., Dutra, R. P. S., Nascimento, R. M., Rajesh, S., Fonseca, F. C. & Macedo, D. A. 2015. Synthesis and properties of CuO-doped Ce0.9Gd0.1O2-δ electrolytes for SOFCs. *Ceramics International 41*(3): 4161–4168. DOI:https://doi.org/10.1016/j.ceramint.2014.12.093.

Menzler, N. H., Tietz, F., Uhlenbruck, S., Buchkremer, H. P. & Stöver, D. 2010. Materials and manufacturing technologies for solid oxide fuel cells. *Journal of Materials Science 45*(12): 3109–3135. DOI:https://doi.org/10.1007/s10853-010-4279-9.

Muda, R., Ahmad, S., Azmi, M. A., Taib, N. & Taib, H. 2019. Characterisation of silica derived from rice husk ash and nickel oxide at different composition and temperatures. *International Journal of Materials and Product Technology 59*(2): 91–101. DOI:https://doi.org/10.1504/IJMPT.2019.102614.

Naceur, H., Megriche, A. & El Maaoui, M. 2014. Effect of sintering temperature on microstructure and electrical properties of Sr1−x(Na0.5Bi0.5)xBi2Nb2O9 solid solutions. *Journal of Advanced Ceramics 3*(1): 17–30. DOI:https://doi.org/10.1007/s40145-014-0089-x.

Nicholas, J. D. & De Jonghe, L. C. 2007. Prediction and evaluation of sintering aids for Cerium Gadolinium Oxide. *Solid State Ionics 178*(19–20): 1187–1194. DOI:https://doi.org/10.1016/j.ssi.2007.05.019.

Palmero, P. 2015. Structural ceramic nanocomposites: A review of properties and powders' synthesis methods. *Nanomaterials 5*(2): 656–696. DOI: https://doi.org/10.3390/nano5020656.

Preethi, S., Abhiroop, M. & Suresh Babu, K. 2019. Low temperature densification by lithium co-doping and its effect on ionic conductivity of samarium doped ceria electrolyte. *Ceramics International 45*(5): 5819–5828. DOI:https://doi.org/10.1016/j.ceramint.2018.11.251.

Rödel, J., Kounga, A. B. N., Weissenberger-Eibl, M., Koch, D., Bierwisch, A., Rossner, W., Hoffmann, M. J., Danzer, R. & Schneider, G. 2009. Development of a roadmap for advanced ceramics: 2010-2025. *Journal of the European Ceramic Society 29*(9): 1549–1560. DOI:https://doi.org/10.1016/j.jeurceramsoc.2008.10.015.

Santos, T. H., Grilo, J. P. F., Loureiro, F. J. A., Fagg, D. P., Fonseca, F. C. & Macedo, D. A. 2018. Structure, densification and electrical properties of Gd3+ and Cu2+ co-doped ceria solid electrolytes for SOFC applications: Effects of Gd2O3 content. *Ceramics International 44*(3): 2745–2751. DOI:https://doi.org/10.1016/j.ceramint.2017.11.009.

Shi, H., Su, C., Ran, R., Cao, J. & Shao, Z. 2020. Electrolyte materials for intermediate-temperature solid oxide fuel cells. *Progress in Natural Science: Materials International 30*(6): 764–774. DOI:https://doi.org/10.1016/j.pnsc.2020.09.003.

Sturm, S. & Jančar, B. 2014. Microstructure Characterization of Advanced Ceramics. *Advanced Ceramics for Dentistry* 151–172. DOI:https://doi.org/10.1016/B978-0-12-394619-5.00008-0.

Sudarsan, P. & Krishnamoorthy, S. B. 2018. Grain boundary scavenging through reactive sintering of strontium and iron in samarium doped ceria electrolyte for ITSOFC applications. *Materials Research Bulletin*, *100:* 446–457. DOI:https://doi.org/10.1016/j.materresbull.2017.12.047.

Tian, N., Qu, Y., Men, H., Yu, J., Wang, X. & Zheng, J. 2020. Properties of Ce0.85Sm0.15O2-δ-CuO electrolytes for intermediate-temperature solid oxide fuel cells. *Solid State Ionics 351*(July 2019). DOI:https://doi.org/10.1016/j.ssi.2020.115331.

Toor, S. Y. & Croiset, E. 2020. Reducing sintering temperature while maintaining high conductivity for SOFC electrolyte: Copper as sintering aid for Samarium Doped Ceria. *Ceramics International 46*(1): 1148–1157. DOI:https://doi.org/10.1016/j.ceramint.2019.09.083.

Varela, J. A., Cerri, J. A., Leite, E. R., Longo, E., Shamsuzzoha, M. & Bradt, R. C. 1999. Microstructural evolution during sintering of CoO doped SnO2 ceramics. *Ceramics International 25*(3): 253–256. DOI:https://doi.org/10.1016/S0272-8842(98)00032-7.

Villas-Boas, L. A., Figueiredo, F. M. L., De Souza, D. P. F. & Marques, F. M. B. 2014. Zn as sintering aid for ceria-based electrolytes. *Solid State Ionics*, *262:* 522–525. DOI:https://doi.org/10.1016/j.ssi.2013.11.002.

Wang, F., Lyu, Y., Chu, D., Jin, Z., Zhang, G. & Wang, D. 2019. The electrolyte materials for SOFCs of low-intermediate temperature: review. *Materials Science and Technology (United Kingdom) 35*(13): 1551–1562. DOI:https://doi.org/10.1080/02670836.2019.1639008.

Wang, Z., Comyn, T. P., Ghadiri, M. & Kale, G. M. 2011. Maltose and pectin assisted sol-gel production of Ce0.8Gd 0.2O1.9 solid electrolyte nanopowders for solid oxide fuel cells. *Journal of Materials Chemistr*, *21*(41): 16494–16499. DOI:https://doi.org/10.1039/c1jm12344k.

Yahya, S. M., Azmi, A., Idris, M. I., Yunos, M. Z., Mahzan, S., Ahmad, S. & Taib, H. 2014. Short review: Role of metal oxides as filler in polysiloxane sheet composite. *Applied Mechanics and Materials 465–466*, 27–31. DOI:https://doi.org/10.4028/www.scientific.net/AMM.465-466.27.

Yin, S., Li, M., Zeng, Y., Li, C., Chen, X. & Ye, Z. 2014. Study of Sm0.2Ce0.8O1.9 (SDC) electrolyte prepared by a simple modified solid-state method. *Journal of Rare Earths 32*(8): 767–771. DOI:https://doi.org/10.1016/S1002-0721(14)60138-1.

Yoshida, H. & Inagaki, T. 2006. Effects of additives on the sintering properties of samaria-doped ceria. *Journal of Alloys and Compounds 408–412*(December 2004): 632–636. DOI:https://doi.org/10.1016/j.jallcom.2004.12.155.

Yusop, U. A., Huai, T. K., Abd.rahman, H., Baharuddin, N. A. & Raharjo, J. 2020. Electrochemical performance of barium strontium cobalt ferrite-samarium doped ceria-argentum for low temperature solid oxide fuel cell. *Materials Science Forum 991 MSF:* 94–100. DOI:https://doi.org/10.4028/www.scientific.net/MSF.991.94.

Zajac, W., Suescun, L., Świerczek, K. & Molenda, J. 2009. Structural and electrical properties of grain boundaries in Ce0.85Gd0.15O1.925 solid electrolyte modified by addition of transition metal ions. *Journal of Power Sources 194*(1): 2–9. DOI:https://doi.org/10.1016/j.jpowsour.2008.12.020.

Zakaria, Z., Awang Mat, Z., Abu Hassan, S. H. & Boon Kar, Y. 2020. A review of solid oxide fuel cell component fabrication methods toward lowering temperature. *International Journal of Energy Research 44*(2: 594–611. DOI:https://doi.org/10.1002/er.4907.

Zhang, T., Hing, P., Huang, H. & Kilner, J. 2002. Sintering and grain growth of CoO-doped CeO 2 ceramics. *Journal of the European Ceramic Society 22*(1): 27–34. DOI:https://doi.org/10.1016/S0955-2219(01)00240-0.

Zhang, T. S., Ma, J., Kong, L. B., Chan, S. H., Hing, P. & Kilner, J. A. 2004. Iron oxide as an effective sintering aid and a grain boundary scavenger for ceria-based electrolytes. *Solid State Ionics 167*(1–2): 203–207. DOI:https://doi.org/10.1016/j.ssi.2004.01.006.

Zhang, X., Decès-Petit, C., Yick, S., Robertson, M., Kesler, O., Maric, R. & Ghosh, D. 2006. A study on sintering aids for Sm0.2Ce0.8O1.9 electrolyte. *Journal of Power Sources* 162(1): 480–485. DOI:https://doi.org/10.1016/j.jpowsour.2006.06.061.

Zhu, T., Lin, Y., Yang, Z., Su, D., Ma, S., Han, M. & Chen, F. 2014. Evaluation of Li2O as an efficient sintering aid for gadolinia-doped ceria electrolyte for solid oxide fuel cells. *Journal of Power Sources* 261*:* 255–263. DOI:https://doi.org/10.1016/j.jpowsour.2014.03.010.